Cell, Vol. 108, 17–29, January 11, 2002, Copyright ©2002 by Cell Press

The Novel Zinc Finger-Containing Transcription Factor Osterix Is Required for Osteoblast Differentiation and Bone Formation

Kazuhisa Nakashima,[2] Xin Zhou,[2] Gary Kunkel,[3] Zhaoping Zhang, Jian Min Deng, Richard R. Behringer, and Benoit de Crombrugghe[1]
Department of Molecular Genetics and Program in Genes and Development
M. D. Anderson Cancer Center
University of Texas
1515 Holcombe Boulevard
Houston, Texas 77030

Summary

We have identified a novel zinc finger-containing transcription factor, called Osterix (Osx), that is specifically expressed in all developing bones. In *Osx* null mice, no bone formation occurs. In endochondral skeletal elements of *Osx* null mice, mesenchymal cells, together with osteoclasts and blood vessels, invade the mineralized cartilage matrix. However, the mesenchymal cells do not deposit bone matrix. Similarly, cells in the periosteum and in the condensed mesenchyme of membranous skeletal elements cannot differentiate into osteoblasts. These cells do, however, express *Runx2/Cbfa1*, another transcription factor required for bone formation. In contrast, *Osx* is not expressed in *Runx2/Cbfa1* null mice. Thus, Osx acts downstream of Runx2/Cbfa1. Because *Osx* null preosteoblasts express typical chondrocyte marker genes, we propose that *Runx2/Cbfa1*-expressing preosteoblasts are still bipotential cells.

Introduction

The development of vertebrate endoskeletons is initially controlled by molecular signals that provide patterning information to the mesenchyme in order to generate primordia of individual skeletal elements (Tickle, 1995; Johnson and Tabin, 1997). These signals outline the three-dimensional coordinates that determine the shape of mesenchymal condensations. Among the molecules that pattern skeletal elements are secreted polypeptides of the Hedgehog, Wnt, and FGF families, and of the TGF-β superfamily, as well as transcription factors of the Pax, Hox, homeodomain-containing, bHLH, and Forkhead families (Karsenty, 1999; DeLise et al., 2000; Olsen et al., 2000). In membranous skeletal elements, cells in condensations differentiate into osteoblasts, whereas in endochondral skeletal elements, cells in condensations differentiate into chondrocytes to form the cartilages that will later be replaced by bones. It has been suggested that both chondrocytes and osteoblasts derive from a common precursor (Fang and Hall, 1997).

Chondrocytes deposit a cartilage-specific extracellular matrix, proliferate, and, in most cases, hypertrophy and die. At the same time, some of the mesenchymal cells surrounding cartilages invade, together with blood vessels and osteoclasts, zones of hypertrophic chondrocytes, differentiate into osteoblasts, and deposit a bone-specific matrix, replacing the degraded cartilage matrix. Interestingly, differentiation of osteoblasts in membranous skeletal elements begins concurrently with that in the endochondral skeleton, suggesting a temporal control synchronizing both modes of bone formation. Three members of the Sox family of transcription factors, Sox9, L-Sox5, and Sox6, which are needed for two successive steps of chondrocyte differentiation, control the fate of the chondrocyte lineage (Bi et al., 1999; Smits et al., 2001).

The transcription factor, Runx2/Cbfa1, a runt family polypeptide, has previously been shown to be required for osteoblast differentiation. In *Runx2/Cbfa1* null mice, osteoblast differentiation is arrested in both the endochondral and intramembranous skeleton (Komori et al., 1997; Otto et al., 1997). In addition, Runx2/Cbfa1 also has a positive role in the differentiation of hypertrophic chondrocytes, a property that should prime the process by which the cartilaginous skeleton is replaced by bone (Inada et al., 1999; Kim et al., 1999; Ueta et al., 2001). Another polypeptide, Indian hedgehog (Ihh), a member of the Hedgehog family of secreted proteins, is required for endochondral but not for intramembranous ossification (St. Jacques et al., 1999). It was proposed that Ihh is needed for the establishment of the osteogenic portion of the perichondrium/periosteum acting upstream of Runx2/Cbfa1. This and additional roles of Ihh coordinate several critical events in endochondral bone formation.

Establishment of cell lineages involves several differentiation steps. For instance, in the differentiation of myoblasts (Black and Olson, 1998), adipocytes (Rosen and Spiegelman, 2000) and chondrocytes, distinct transcription factors control discrete differentiation steps. Hence, we have postulated that in the differentiation of osteoblasts, other transcription factors, in addition to Runx2/Cbfa1, might be required. To identify such transcription factors, we have designed a simple screen to isolate cDNAs that are osteoblast-specific. This screen has identified a novel zinc finger-containing transcription factor called Osterix (Osx) that is expressed in osteoblasts of all endochondral and membranous bones. In *Osx* null mutant mice, no endochondral and no intramembranous bone formation occur. Arrest in osteoblast differentiation occurs at a later step than in *Runx2/Cbfa1* null mice.

Results

Cloning of cDNA for *Osterix*

When C2C12 skeletal muscle progenitor cells become confluent in culture, they fuse into typical multinucleated

[1] Correspondence: bdecromb@mdanderson.org
[2] These authors made equal contributions to this work.
[3] Present address: Department of Biochemistry and Biophysics, Texas A&M University, College Station, Texas 77843

myotubes. However, upon BMP-2 addition, these cells transdifferentiate into osteoblasts (Katagiri et al., 1994). To identify potential osteoblast-specific proteins, we used a two-step screen consisting of a PCR-based suppression-subtractive hybridization followed by differential hybridization. A cDNA clone from this screen hybridized with a 3 kb RNA that was induced early after BMP-2 addition to C2C12 cells, at about the same time that *Runx2/Cbfa1* RNA could be detected, but much earlier than RNA for the late osteoblast marker osteocalcin was expressed (for detailed results, see Supplemental Data at http://www.cell.com/cgi/content/full/108/1/17/DC1). *Osx* was expressed in ROS17/2.8 and MC3T3-E1 osteoblast cell lines and in rat chondrosarcoma cells. However, *Osx* was not expressed in Balb3T3 fibroblasts, S194 B cells, and PC12 cells (data not shown).

The *Osx* cDNA obtained by subtraction was used to identify larger cDNAs, the sequences of which showed an open reading frame of 1284 nucleotides and were capable of encoding a 428 amino acid polypeptide with a predicted molecular weight of 44.7 kDa.

To examine the size of the corresponding endogenous polypeptide, antibodies were raised against a 14 amino acid peptide located at the C terminus of the deduced polypeptide sequence. The purified antibodies recognized a 46 kDa protein present in extracts of C2C12 cells treated with BMP-2 but not in extracts of untreated cells. The size of this polypeptide was in agreement with that predicted from the deduced amino acid sequence of Osx, strongly suggesting that our cDNA encoded the full-length Osx polypeptide.

The Osx amino acid sequence predicted the existence of three C2H2-type zinc fingers at the C terminus of Osx. This 85 amino acid zinc finger motif had a high degree of homology with the motifs present in the transcription factors Sp1, Sp3, and Sp4, and had a somewhat lower homology with those in other transcription factors of the Krüppel-like transcription factor family. Upstream of the zinc finger domain was a stretch of basic amino acids similar to those in a region of EGR-1 that has been shown to be important for nuclear localization (Gashler et al., 1993). Therefore, we concluded that Osx was a novel polypeptide with features typical of a transcription factor.

Expression Pattern of *Osx*

To identify the cell types that expressed *Osx* in vivo, we performed in situ hybridization with mouse embryos at various stages of development and with tissues from newborn mice (for detailed results, see Supplemental Data at http://www.cell.com/cgi/content/full/108/1/17/DC1). In brief, *Osx* transcripts were first found transiently in differentiating chondrocytes and in the surrounding perichondrium of E13.5 embryos, but were not detected in the condensed chondrogenic mesenchyme. Rapidly thereafter, transcripts were confined mainly to the peripheral layers of endochondral skeletal elements and were absent from more centrally located chondrocytic cells. At E15.5 and later, strong expression was found in cells associated with all bone trabeculae and in those associated with formation of bone collars. Weak expression was detected in the prehypertrophic zone, but not in other cells of growth plate cartilage. Mesenchymal cells of the tooth germ also showed a positive signal, whereas no expression was detected in the epithelial tissue of the tooth germs and Meckel's cartilage. In 13-day-old mice, expression remained strong in bone trabeculae and in secondary ossification centers. At this stage, cells either within the bone matrix or associated with the inner (endosteum) and outer (periosteum) bone surfaces were positive for *Osx* expression.

Biochemical Characterization of Recombinant Osx

The three zinc finger motif located at the C-terminal part of Osx and its high degree of sequence homology with a similar motif in Sp1, Sp3, and Sp4 strongly suggested that Osx binds DNA. A recombinant Osx polypeptide (amino acids 27–428) was generated by transfection of an *Osx* expression vector into COS-7 cells. One major complex was formed with extracts of *Osx*-transfected cells and a double-stranded oligonucleotide containing a consensus Sp1 binding site (Figure 1A, lanes 9–13). Formation of this complex was abolished by incubation with anti-C-terminal Osx antibodies (Figure 1A, lanes 14–16), but binding to DNA was restored by addition of the C-terminal peptide that was used to generate these antibodies (Figure 1A, lanes 17 and 18), indicating that the DNA-protein complex consisted of recombinant Osx and labeled probe. Osx also bound strongly but with different efficiencies to several other functional G/C-rich sequences, including those of the EKLF consensus site and Sp1-like sequences in the *Col1a1* and *Col2a1* promoters (Figure 1B). G to T mutations in two adjacent residues of a G/C-rich binding site abolished Osx binding (data not shown). Thus, our results suggested that Osx was a sequence-specific DNA binding protein.

To verify whether Osx contained a transcription activation domain, various segments of the protein were fused in frame with the DNA binding domain of the yeast transcription factor GAL4. The expression vectors were transfected into COS-7 cells with a reporter gene containing five tandem GAL4 binding sites. A plasmid expressing the GAL4 DNA binding domain was transfected as a control. Figure 1C shows that the segment containing residues 27–270 and the smaller proline/serine-rich segment from residues 27–192 provided strong transcriptional activation. Neither the near full-length protein (residues 27–428) nor the zinc finger region of Osx (residues 293–428) had appreciable transcriptional activity when fused to GAL4. Figure 1D shows that the expression levels of the fusion polypeptides were similar except for the fusion containing residues 27–192, which was expressed at a lower level. Thus, our experiments indicated that Osx contained a strong transcription activation domain.

To test the subcellular localization of Osx polypeptides, COS-7 cells were transfected with a Flag-tagged *Osx* expression vector and were examined by immunofluorescence using anti-Flag antibodies. In these experiments, Osx's localization was restricted to the nucleus (Figure 1E). Thus, on the basis of Osx's DNA binding properties, its transcription activation domain, and its subcellular localization, we concluded that it had the properties of a typical transcription factor.

To test whether Osx could activate typical osteoblast

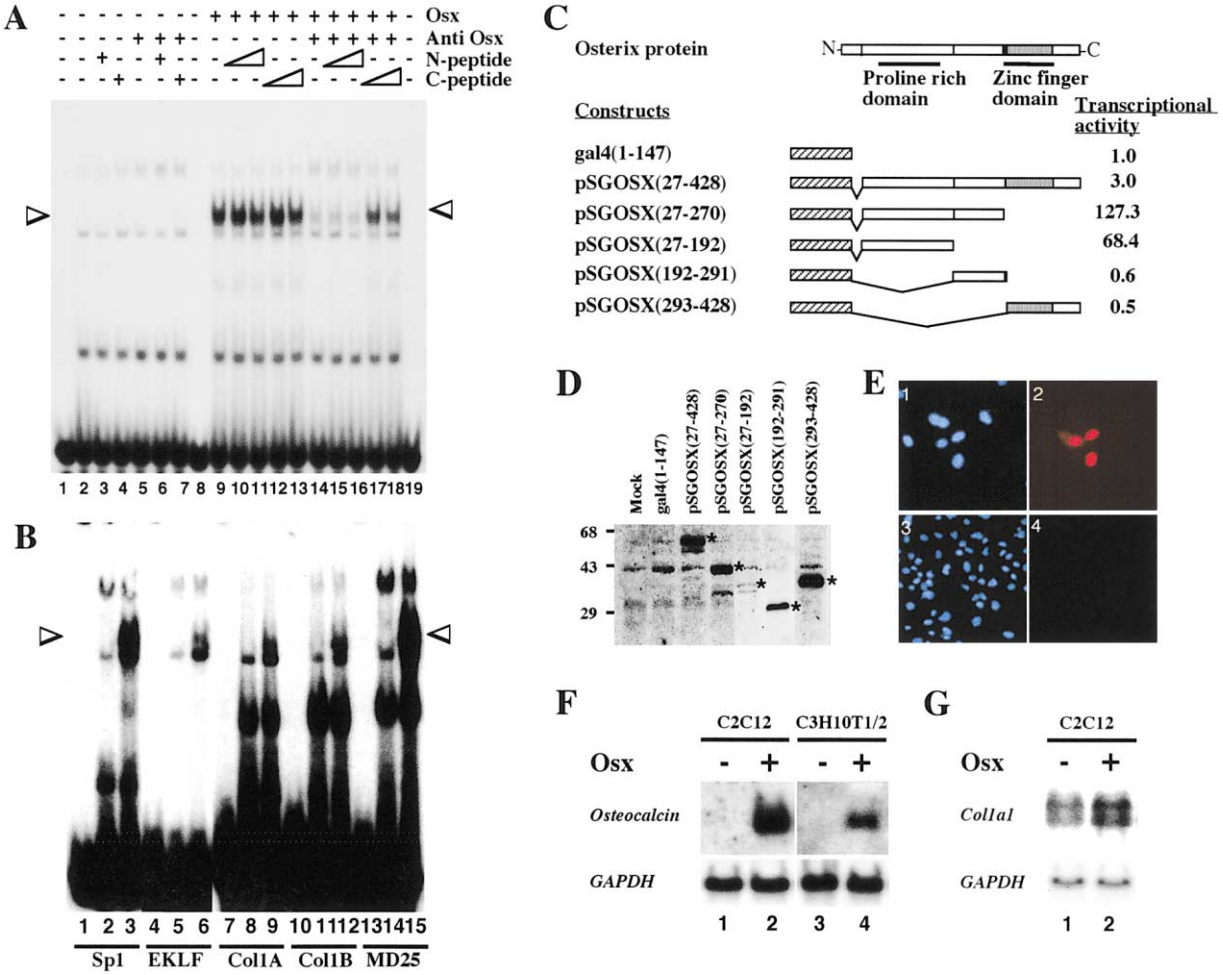

Figure 1. DNA Binding, Transcriptional Activity, and Cellular Localization of Osx

(A) EMSA using a consensus Sp1 binding site as probe, without (lanes 1, 8, and 19) or with extracts of COS-7 cells transfected with empty expression vector (lanes 2–7) or an *Osx* expression vector (lanes 9–18). DNA binding in the absence (lanes 1–4, 8, 9–13, and 19) or presence (lanes 5–7 and 14–18) of purified anti-Osx antibodies. To show antibody specificity, the binding reaction was performed in the presence of N-terminal peptide (1.5 μg: lanes 3, 6, 11, and 16, 0.5 μg: lanes 10 and 15) or C-terminal peptide (1.5 μg: lanes 4, 7, 13, and 18, 0.5 μg: lanes 12 and 17), which was used to generate antibodies. Arrows indicate specific complexes containing recombinant Osx proteins.

(B) Labeled, double-stranded oligonucleotides containing different G/C-rich sequences were used as probes, without (lanes 1, 4, 7, and 13) or with extracts of COS-7 cells transfected with an empty expression vector (lanes 2, 5, 8, and 14) or an *Osx* expression vector (lanes 3, 6, 8, and 15). DNA sequences of C-rich strands of oligonucleotides used were: Sp1, 5′-GCT CGC CCC GCC CCG ATC GAA T-3′; EKLF, 5′-CGT AGA GCC ACA CCC TGA AGG-3′; Col1a1A, 5′-TCC ACC CAG CGC GCC CCC CCT CCC GCA A-3′; Col1a1B, 5′-CCT TCC TTT CCC TCC TCC CCC CTC TTC G-3′; MD25, 5′-TAA CCT GAG ACC CCG CCC CCG GAG CCC-3′.

(C) Segments of Osx were fused in frame with the GAL4 DNA binding domain and transiently transfected into COS-7 cells with a luciferase-reporter plasmid. Numbers show relative luciferase activity after normalization for β-gal activity.

(D) Western blot performed to monitor expression of GAL4-fusion polypeptides in COS-7 cells using antibodies to the DNA binding domain of GAL4.

(E) Nuclear localization of the recombinant Osx. Flag-tagged Osx protein was expressed in COS-7 cells and immunostained with (panel 2) or without (panel 4) anti-Flag antibodies, followed by incubation with Texas red-conjugated anti-mouse IgG antibodies. DAPI staining (panels 1 and 3) was performed to visualize nuclei in the identical fields shown in panels 2 and 4. Panels 1 and 2: 20×, Panels 3 and 4: 10×.

(F) C2C12 and C3H10T1/2 cells were transfected with an *Osx* expression vector (3 μg), and incubated for 48 hr. Northern hybridization was performed with *osteocalcin* and *GAPDH* probes.

(G) C2C12 cells were transfected with an *Osx* expression vector (3 μg), and incubated for 24 hr. Northern hybridization was performed with *Col1a1* and *GAPDH* probes.

genes, we transfected an *Osx* expressing vector into both C2C12 and C3H10T1/2 cells. Our results showed that Osx produced an induction of *osteocalcin* RNA in both cell types (Figure 1F). In addition, Osx activated *type I collagen* gene expression in C2C12 cells (Figure 1G).

To determine the chromosomal location of the *Osx* gene in the mouse genome, a interspecific mapping panel of 94 DNA samples obtained from The Jackson Laboratory was analyzed. The results indicated that the *Osx* gene (symbol *Sp7*) was located on mouse chromo-

some 15 between *Wnt10b* and *Itga5*. Based on this chromosomal location, the predicted syntenic region for the human *SP7* gene was chromosome 12q13. No inherited skeletal disease has been mapped to this region.

Inactivation of the *Osx* Gene

To better understand the function of Osx, we inactivated the *Osx* gene in mouse embryonic stem (ES) cells using homologous recombination. The *Osx* gene contained only two exons. Except for the DNA sequence encoding the seven N-terminal amino acids of Osx, the rest of the coding sequence was present in exon 2. Our targeting strategy (Figure 2A), which deleted most of the coding sequence of exon 2, functionally inactivated the *Osx* gene. Insertion of the *lacZ* gene predicted that expression of β-galactosidase (β-gal) would follow an *Osx* expression pattern. Mice were genotyped by both Southern hybridization (Figure 2B) and by PCR amplification (Figure 2C). The absence of *Osx* RNA in northern blot experiments using a probe 3′ to the *Osx* deletion in E17.5 homozygous mutant embryo indicated that the mutation was a null mutation (Figure 2D). Heterozygous *Osx* mutant mice were normal and fertile. Homozygous *Osx* mutant mice, which were recovered with the expected Mendelian ratio, died in the immediate postnatal period. These mice had difficulty in breathing, rapidly became cyanotic, and died within 15 min of birth. Newborn homozygous mutant mice showed severe inward bending of forelimbs and hindlimbs (Figure 2E, arrows).

X-gal staining of E14.5 embryos showed that the pattern of β-gal expression was very similar in heterozygous and homozygous *Osx* mutants and faithfully reproduced the pattern of expression of the endogenous *Osx* gene (Figure 2F). X-gal staining was undetectable in E12.5 embryos, but it was clearly evident by E13.5 (data not shown). Skeletal preparations of E15.5 *Osx* null embryos showed that cartilage developed well and prefigured all endochondral skeletal elements, as observed by alcian blue staining. No bending was observed in the forelimbs and hindlimbs at this stage of development (Figure 2G, arrows). These results indicate that no patterning defects were present in *Osx* null mutant embryos.

However, practically no mineralization was detected by alizarin red staining in E15.5 *Osx* null mutant embryos (Figure 2G). Staining of skeletal preparations from newborn homozygous mutant mice with alcian blue and alizarin red indicated a virtual absence of mineralization in all facial and skull bones formed by intramembranous ossification (Figure 2H), whereas supraoccipital, exoocipital, basioccipital, basisphonoid, and sphenoid bones of the chondrocranium (Figure 2I), which are formed by endochondral ossification, were stained by alizarin red. The clavicles were extremely hypoplastic (Figure 2J). Other skeletal elements formed by endochondral ossification, including the ribs, limb bones, and vertebrae, were hypoplastic, bent, and often deformed, but no irregular fusion of joints occurred. Comparison of alizarin red staining of different endochondral skeletal elements indicated that mineralization was delayed and took place within cartilage of the mutant mice, suggesting that no bone collar formed in the mutants (Figures 2G, 2K, 2L, 2M, and 2N). This is best illustrated when the wild-type and mutant hyoid skeletal elements were compared (Figures 2L and 2M). The defects in mineralization were already visible in E14.5 *Osx* null mutants (data not shown), the same time when ossification centers first began to form in wild-type embryos.

Histological Analysis of *Osx* Null Mutants

Wild-type E16.5 mandible and maxilla showed typical trabeculae and the presence of mineralization, as detected by von Kossa's staining (Figures 3A1 and 3B1). In the null mutants, however, only condensed mesenchymal cells were present at these locations, and no bone trabeculae or mineralization were detectable (Figures 3A2 and 3B2). Identical observations were made between wild-type and mutant mice in other membranous skeletal elements, such as frontal bones (data not shown). The cellular organization of the tooth germ, Meckel's cartilage, and the musculus masseter was indistinguishable between wild-type and mutant mice. The humerus of E16.5 wild-type mice displayed typical cellular organization of growth plate chondrocytes and characteristic bone trabeculae of the ossification zone, as well as mineralization of the bone trabeculae, collars, and the zone of hypertrophic chondrocytes close to the chondroosseous junction (Figures 3A3 and 3B3). In contrast, the humerus of E16.5 *Osx* null mutants had no bone trabeculae. Instead, a wedge-shaped mesenchyme containing red blood cells emerged from the central part of the periosteum (Figure 3A4), implying that blood vessels were also present. No mineralization was seen in the wedge-shaped mesenchyme. Similarly, no mineral deposition occurred in the inner layer of the periosteum/perichondrium, indicating that no bone collar formed. However, mineral deposition was present in the alcian blue-stained matrix of the zone of the hypertrophic chondrocytes adjacent to the wedge-shaped mesenchyme (Figure 3B4), accounting for the alizarin red staining observed in whole-mount skeletal preparations at this time of embryonic development (data not shown). The abnormalities in the humerus were present in all other endochondral skeletal elements (data not shown).

In E14.5 *Osx* null membranous skeletal elements, condensed mesenchymal cells were β-gal positive. Since these cells occupied the same space as they did in wild-type embryos, they had migrated to their correct location in the mutants and had presumably responded to the same signals as did wild-type cells (Figures 3C1–3C4). Mesenchymal cells in the periosteum/perichondrium and in the wedge-shaped mesenchyme of the *Osx* null humerus also expressed β-gal (Figure 3C4). These β-gal expression patterns were reproduced in E17.5 heterozygous and homozygous mutant mice (data not shown).

Expression of Osteoblast Markers

To better characterize the abnormalities of *Osx* mutant mice, we examined the expression of several early and late osteoblast marker genes by in situ hybridization. Type I collagen, which is the most abundant protein in bone matrix (Bilezikian et al., 1996), is an early marker of osteoblast differentiation. In E16.5 wild-type embryos, *Col1a1* RNA levels were much higher in osteoblasts than in fibroblasts of the skin and mesenchymal cells (Figures

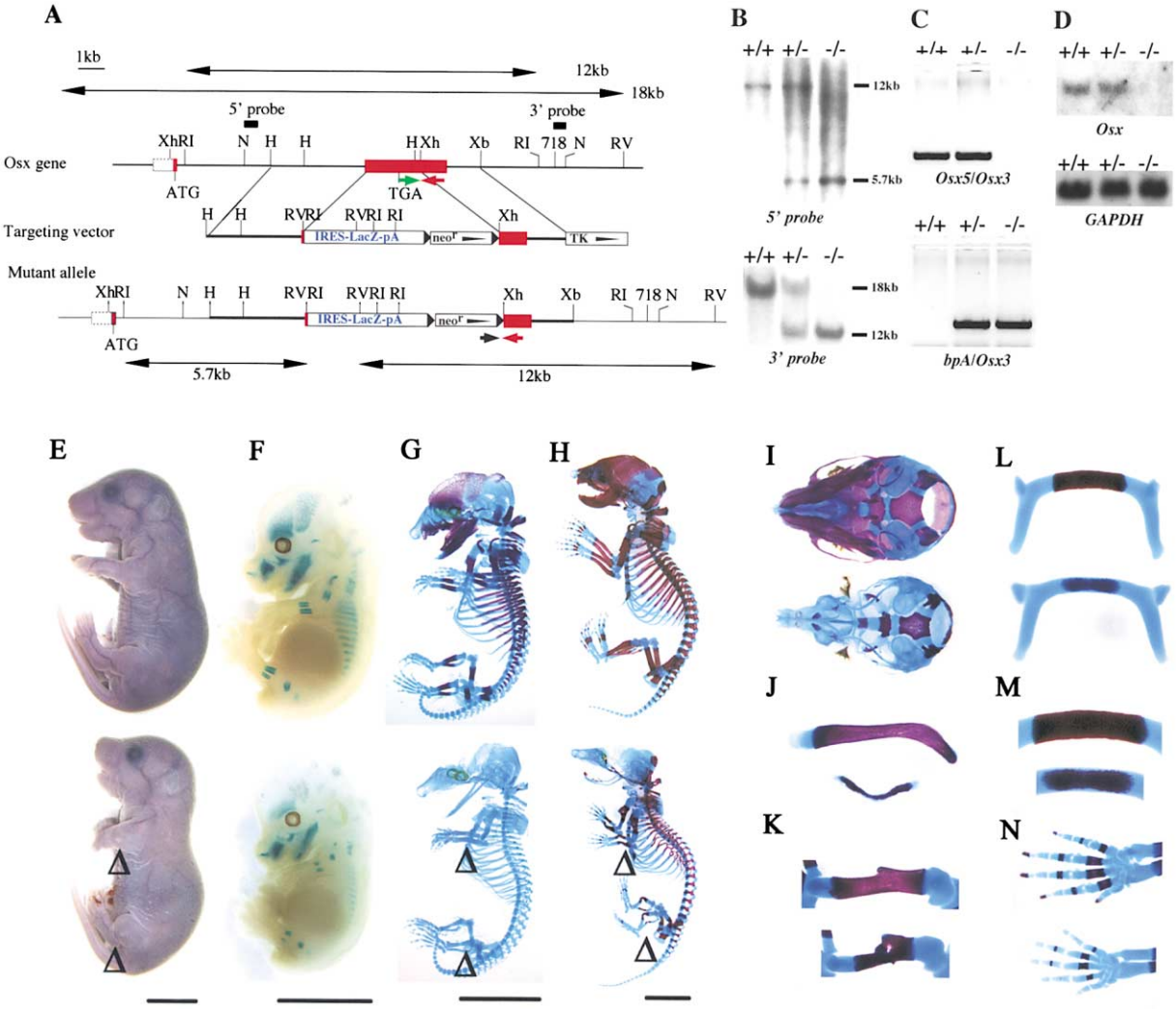

Figure 2. Generation of *Osx* Mutant Mice and Analysis of Their Skeletal Phenotype

(A) Structure of the genomic *Osx* locus, targeting vector, and mutated allele after homologous recombination. Exons are depicted as closed boxes. IRES-LacZ/PGK-neo casetttes are depicted as open boxes. Xh, XhoI; N, NheI; H, HindIII; Xb, XbaI, RI, EcoRI; 718, Asp718; RV, EcoRV.

(B) Southern blot analysis of fetal genomic DNA. Genomic DNA isolated from the tail was digested with EcoRI or EcoRV and then hybridized with the 5′ probe or the 3′ probe, respectively. The wild-type and mutant alleles were detected as 12 kb and 5.7 kb fragments, respectively, with the 5′ probe, and as 18 kb and 12 kb fragments with the 3′ probe.

(C) PCR genotyping was performed using two sets of primers: Osx5 (green arrow in A) and Osx3 (red arrow in A) for the wild-type allele and bpA (black arrow in A) and Osx3 for the mutant allele.

(D) Northern blot analysis of *Osx* expression in wild-type and mutant mice. Ten micrograms of total RNA isolated from E17.5 wild-type, heterozygous mutant and homozygous mutant embryos were hybridized with a 0.5 kb *Osx* cDNA probe.

In (E) and (G)–(N), upper panels show wild-type mice and lower panels homozygous mutant mice. Bars in (E)–(H) indicate 5 mm.

(E) Gross appearance of newborn embryos. The homozygous mutants show inward bending of limbs (arrows).

(F) β-gal activity in heterozygous (upper) and homozygous mutant (lower) mice at E14.5.

(G) Skeletons of E15.5 mice stained by alcian blue followed by alizarin red. Limbs of mutant embryos show no bending (arrows).

(H) Skeletons of newborn mice. Distal limbs of mutant mice show bending (arrows).

(I–N) Ventral view of skulls (I), clavicles (J), humeri (K), hyoid bones (L) and a higher magnification of the mineralized part of the hyoid bones (M), and palms (N).

3D1 and 3D3). In contrast, in *Osx* null mutant embryos, the *Col1a1* RNA levels in the condensed mesenchyme of the membranous skeleton and in the periosteum and the wedge-shaped mesenchyme of the endochondral skeleton were severely reduced, expressed at levels similar to those in skin fibroblasts (Figures 3D2 and 3D4). Expression of the gene for Bone Sialoprotein (BSP), another early marker of osteoblast differentiation (Chen et al., 1992), was seen in all bones of wild-type embryos (Figures 3E1 and 3E3). In contrast, it was undetectable in the condensed mesenchyme of membranous and endochondral skeletal elements and in the periosteum of *Osx* null mutants (Figures 3E2 and 3E4). Transcripts for osteonectin and osteopontin, two other osteoblast markers, were undetectable in the condensed mesenchyme substituting for osteoblasts in E16.5 *Osx* null embryos

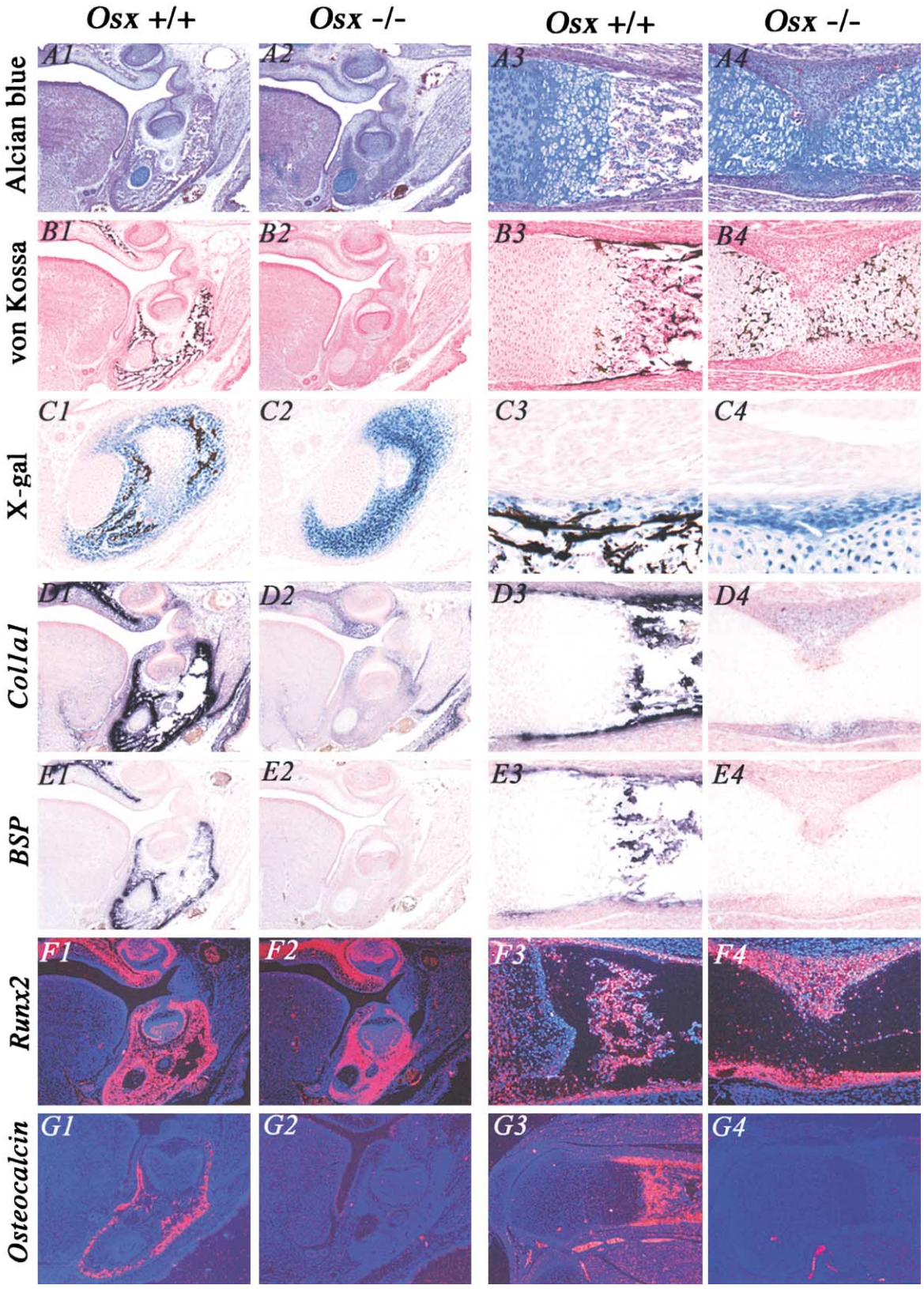

Figure 3. Histological Examination of Mutant Mice

Panels (1) and (2) show coronal sections of the skull, and panels (3) and (4) show the humerus. Panels (1) and (3) show wild-type embryos, and panels (2) and (4) show homozygous mutant embryos. In panel (C), (C1) and (C3) show heterozygous mutant embryos.

(A) View of the maxilla, mandible, and humerus at E16.5. Sections were stained with alcian blue and counterstained with hematoxylin and

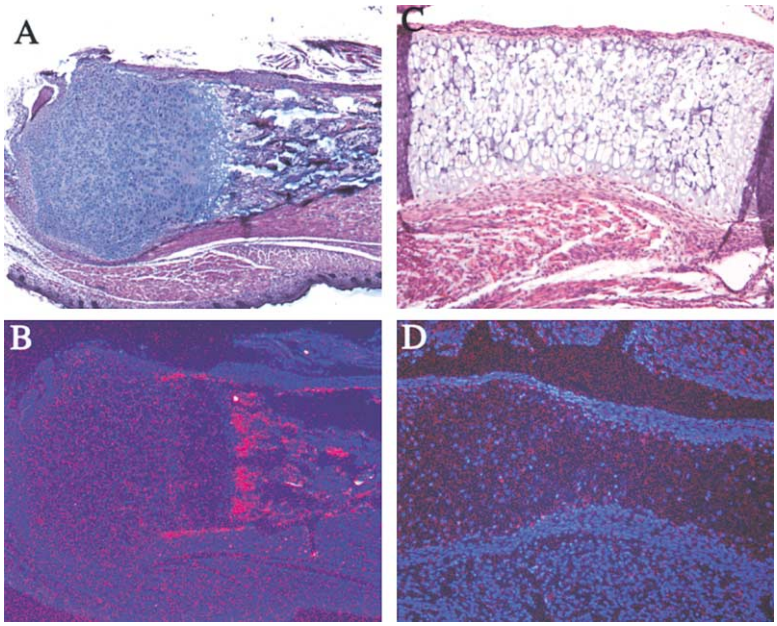

Figure 4. Expression of *Osx* in *Runx2/Cbfa1* Null Mice

(A) The proximal growth plate of the humerus of wild-type-mice stained with alcian blue, hematoxylin, and Treosin. (C) The middle part of the tibia of *Runx2/Cbfa1* null mice stained with hematoxylin and eosin. Neighboring sections of wild-type humerus (B) and of *Runx2/Cbfa1* null tibia (D) were hybridized with the *Osx* probe. Chondrocytes and cells in thin perichondrium showed no expression of *Osx* in *Runx2/Cbfa1* null mice.

(data not shown). In wild-type E16.5 embryos, *Runx2/Cbfa1*, which is required for osteoblast differentiation, was expressed in all osteoblasts. In *Osx* null mutants, *Runx2/Cbfa1* was expressed at levels comparable to those found in wild-type osteoblasts in the condensed mesenchymal cells of membranous skeletal elements and in the periosteum and the wedge-shaped mesenchyme of the endochondral skeleton (Figures 3F1–3F4). These same results had already been observed in E14.5 embryos, the developmental stage when ossification was first initiated in wild-type embryos (data not shown).

In E18.5 *Osx* null embryos, expression of RNA for osteocalcin, a late osteoblast marker and the most cell-specific one, was also absent in endochondral and membranous skeletal elements (Figures 3G2 and 3G4). In addition, transcripts for *BSP*, *osteonectin*, and *osteopontin* were absent in the periosteum of E18.5 *Osx* mutants (data not shown). Thus, early markers of osteoblast differentiation were not expressed at late stages of mouse development. We concluded that in *Osx* null embryos, despite the presence of *Runx2/Cbfa1* expression at levels comparable to those in wild-type embryos, both early and late markers of osteoblast differentiation were absent and, thus, osteoblast differentiation was completely arrested.

Normal levels of *Runx2/Cbfa1* expression in *Osx* null mutants indicated that Osx was not required for *Runx2/Cbfa1* expression and suggested either that Runx2/Cbfa1 and Osx belonged to two independent pathways that controlled osteoblast differentiation or that both transcription factors were functioning in the same pathway. To distinguish between these two possibilities, we asked whether *Osx* was expressed in *Runx2/Cbfa1* null mice. Figure 4D shows that no *Osx* transcripts were detected in the periosteum of endochondral skeletal elements of *Runx2/Cbfa1* null mice. Thus, these results indicated that Osx was downstream of Runx2/Cbfa1 in the pathway of osteoblast differentiation and that Runx2/Cbfa1 was needed for *Osx* expression.

Presence of Osteoclasts in *Osx* Null Mutants

Whereas no invasion of the zone of hypertrophic chondrocyte occurs in *Runx2/Cbfa1* null mice (Figure 4C) (Komori et al., 1997), there was extensive migration of the mesenchymal cells into the mineralized cartilage matrix in *Osx* null mice (Figure 5A). In wild-type mice, osteoblasts produce a typical eosinophilic bone matrix using remnants of the degraded mineralized cartilage septae as a template (Figure 5B). In the E18.5 *Osx* null humerus, remnants of degraded mineralized septae of hypertrophic chondrocytes were clearly visible by alcian blue staining (Figure 5C). In contrast to those in wild-type humerus, these remnants were not surrounded by bone matrix, as detected by Treosin staining.

To determine whether osteoclasts were involved in the degradation of the mineralized cartilage matrix of

Treosin. In mutant mice, densely packed mesenchymal cells surround Meckel's cartilage and tooth germs in the jaws and are present as a wedge-shaped mesenchyme in the humerus.

(B) Staining by von Kossa's method visualizes mineral deposition in the maxilla and mandible and humeri in wild-type and mutant mice at E16.5. Maxilla and mandible show no mineralization in mutant mice. Mineralization of the humerus occurs only within the alcian blue-positive hypertrophic chondrocyte matrix shown in (A). No mineralization was detected in the perichondrium/periosteum layer.

(C) Localization of β-gal-expressing cells in E14.5 embryos. β-gal-expressing cells were stained blue by whole mount X-gal staining and mineral deposition was detected by von Kossa's method. In heterozygous mice, mineral deposition occurs within matrix associated with β-gal-expressing cells (C1 and C3), which is lacking in mutant mice (C2 and C4).

(D–F) Expression of the *Col1a1* gene (D), the *BSP* gene (E), and the *Runx2/Cbfa1* gene (F) in E16.5 embryos.

(G) Expression of the *osteocalcin* gene in embryos at E18.5.

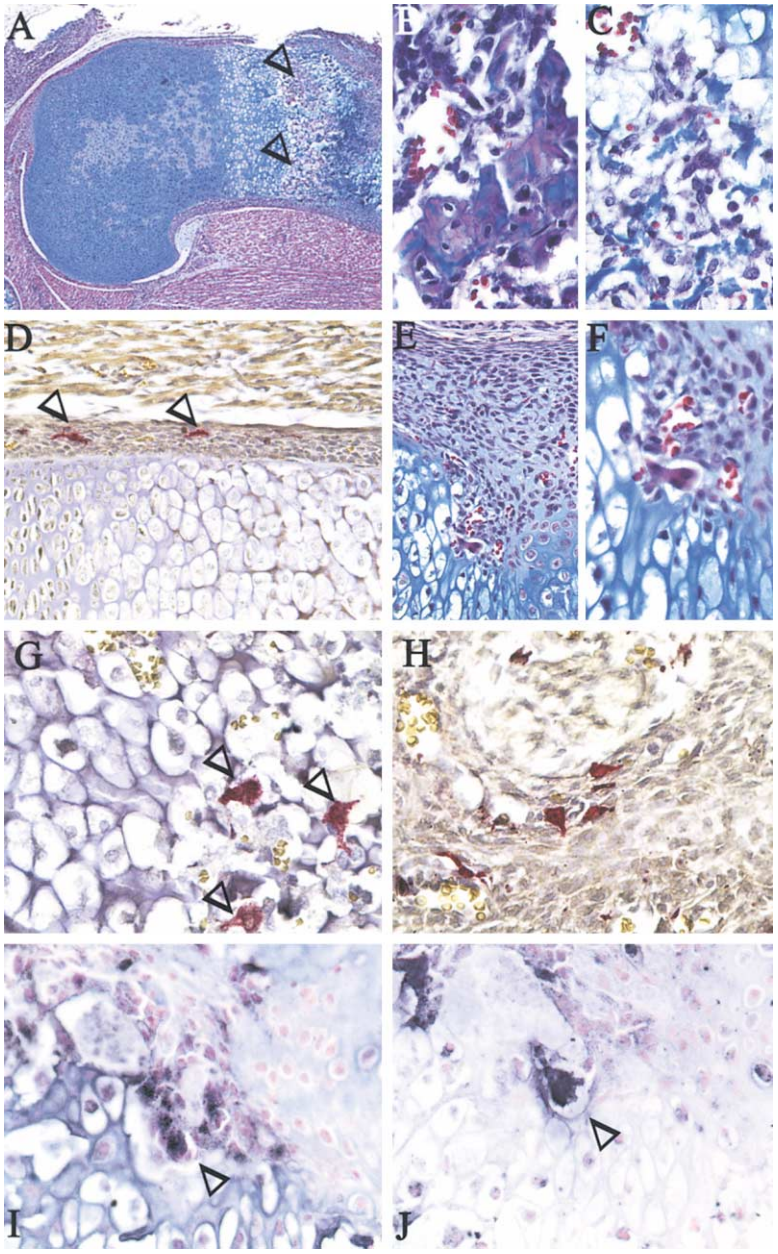

Figure 5. Matrix Degradation and Osteoclastogenesis in *Osx* Null Mice

(A) Alcian blue, hematoxylin, and Treosin staining of the proximal growth plate of the humerus in a newborn *Osx* null mice. Arrows indicate migration of mesenchymal cells.

(B) Alcian blue, hematoxylin, and Treosin staining of a wild-type proximal growth plate of the humerus shows eosinophilic matrix accumulation corresponding to bone matrix deposition around the alcian blue-stained degraded cartilaginous matrix.

(C) No such eosinophilic deposition occurs in the homozygous mutant.

(D) TRAP staining of the humerus of a homozygous mutant at E14.5 reveals TRAP-positive cells in the middle of the fibrous layer of the perichondrium.

(E) At E16.5, eosinophilic cells, together with red blood cells, localize to the interface of the cartilage and the mesenchyme.

(F–J) (F) High magnification of (E): a multinucleated eosinophilic cell extending cellular processes into the cartilage matrix. At E18.5, TRAP-positive cells localize within the cartilage matrix produced by hypertrophic chondrocytes (G) and within the condensed mesenchyme of the mandible (H). Expression of MMP-9 (I) and cathepsin K (J) detected by immunostaining in cells migrating into the cartilage matrix.

Osx null mutants, we examined whether tartrate-resistant acid phosphatase (TRAP)-positive cells were present. In E14.5 *Osx* null embryos, TRAP-positive cells were detected within the periosteum of endochondral skeletal elements (Figure 5D). Figures 5E and 5F show that in the humerus of E16.5 *Osx* null mutants, multinucleated cells were present, together with red blood cells, at the boundary between invading mesenchymal cells and the matrix of hypertrophic chondrocytes. In mutant E18.5 embryos and newborn mice, TRAP-positive cells were found within the degraded hypertrophic cartilage matrix (Figure 5G). Similarly, TRAP-positive multinucleated cells were seen among the mesenchymal cells of the mandibular skeletal element of newborn *Osx* null mice (Figure 5H). MMP-9 (Vu et al., 1998) and cathepsin K (Gowen et al., 1999), which are osteoclast markers, were present in *Osx* null newborn mice, suggesting that the TRAP-positive cells in these mutants were functional osteoclasts (Figures 5I and 5J). These results indicated that, in contrast to the *Runx2/Cbfa1* null mutants in which only mononucleated TRAP-positive cells were seen in the periosteum, multinucleated functional osteoclasts were observed in the cartilage matrix in *Osx* null mutants.

Fate of *Osx* Null Mutant Cells

Given that osteoblast differentiation was arrested in *Osx* null mutant cells and that the cells expressed levels of *Runx2/Cbfa1* comparable to those in wild-type osteoblasts, we asked whether the *Osx* null mutant cells could adopt a different cell fate. This was first suggested by the observation that alcian blue stained the matrix in

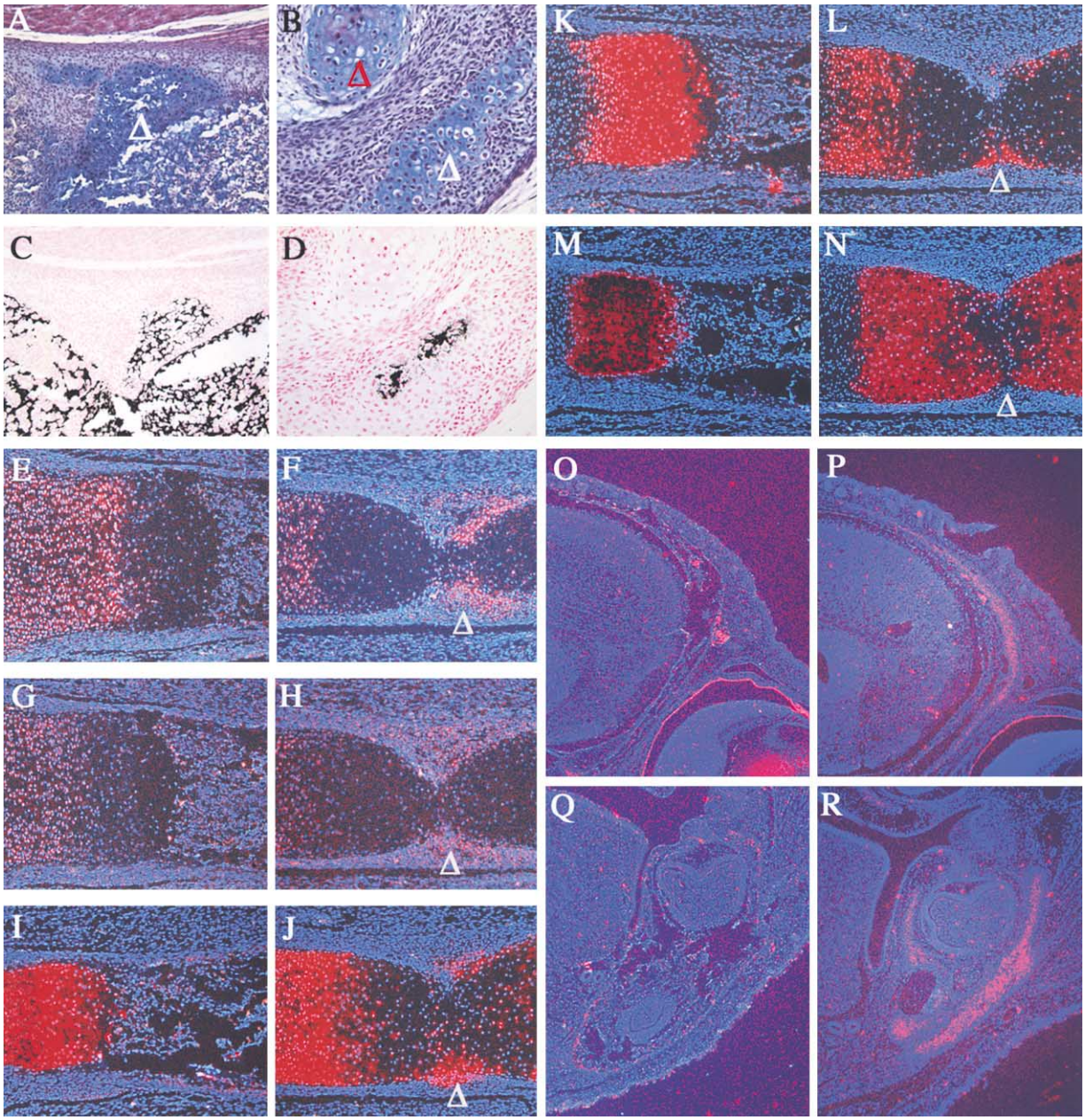

Figure 6. Expression of Chondrocyte Markers in Homozygous Mutant Mice

Alcian blue, hematoxylin, and Treosin staining of the homozygous mutant humerus (A) and the lower jaw (B) at E18.5 showing ectopic differentiation of chondrocytes in condensed mesenchymes. In the humerus, round cells with alcian blue positive matrix (A, arrow) appeared in inner layer of perichondrium. In the lower jaw, an adjacent region of the condensed mesenchyme to the Meckel's cartilage (red arrow) is stained by alcian blue (white arrow). (C) and (D) are neighboring sections of (A) and (B), respectively, stained by von Kossa's method. (E), (G), (I), (K), and (M) show humerus in E16.5 wild-type mice. (O) and (Q) show skull and jaw, respectively, in E18.5 wild-type mice. (F), (H), (J), (L), and (N) show humerus in E16.5 homozygous mice. (P) and (R) show skull and jaw, respectively, in E18.5 homozygous mice. (E and F) Expression of *Sox9*. (G and H) Expression of *Sox5*. (I and J) Expression of *Col2a1*. (M and N) Expression of *Col10a1*. (K, L, O, P, Q and R) Expression of *Ihh*.

the mesenchyme in membranous skeletal primordia and cells in the wedge-like mesenchyme in endochondral skeletal elements of E18.5 *Osx* null embryos (Figures 6A and 6B). Moreover, cells embedded in an alcian blue-stained matrix had a round shape characteristic of chondrocytes. Some of the cells were capable of mineralizing their matrix (Figures 6C and 6D). This also accounted for the small amounts of alizarin red staining seen in the mandibular region outside of the Meckel's cartilage in newborn *Osx* null mice (Figure 2H).

We therefore examined expression of molecular markers of chondrocyte differentiation in the mutant cells in E16.5 null mutant mice. The cells in the wedge-shaped mesenchyme of *Osx* null endochondral skeletal ele-

ments expressed *Sox9*, *Sox5*, *Col2a1*, and *Ihh* transcripts (Figures 6F, 6H, 6J, and 6L). Similarly, *Osx* null membranous skeletal elements showed ectopic expression of these transcripts (Figures 6P and 6R, and data not shown). In the humerus of E16.5 *Osx* null mutants, expression of *Col10a1*, which was seen in hypertrophic chondrocytes of the cartilage growth plate (Figure 6N), was still largely excluded from the cells of the wedge-shaped mesenchyme that ectopically expressed *Sox9*, *Sox5*, *Col2a1*, and *Ihh*. Overall these results indicated that *Runx2/Cbfa1*-expressing *Osx* null cells, which could not differentiate into osteoblasts, acquired a cell fate characterized by the expression of a series of genes that are typical of chondrocytes.

Discussion

Osx Is Essential for Osteoblast Differentiation

Our results established that the novel transcription factor Osx is required for osteoblast differentiation and hence for bone formation. In the absence of Osx, no cortical bone and no bone trabeculae were formed through either intramembranous or endochondral ossification. During normal endochondral bone formation, the degradation of the mineralized cartilage matrix by osteoclasts/chondroclasts and the deposition of a characteristic bone matrix by osteoblasts are tightly coordinated. In endochondral skeletal elements of *Osx* null mutants, mesenchymal cells from the perichondrium/periosteum, together with blood vessels, invaded the mineralized matrix of the zone of hypertrophic chondrocytes. Moreover, the presence of multinucleated osteoclasts in the mineralized cartilage matrix of *Osx* null mutants and degradation of this matrix indicated that osteoclast differentiation and active cartilage matrix degradation were taking place. This was further supported by the demonstration of cells expressing MMP-9 and cathepsin K in the hypertrophic cartilage matrix. However, mesenchymal cells migrating together with osteoclasts and blood vessels could not deposit bone matrix, so no ossification could occur in the matrix of this mesenchyme. Similarly, no ossification took place in the condensed mesenchyme of membranous skeletal elements. The degraded mineralized cartilage matrix and the absence of bone matrix accounted for the severe bending of long bones.

In contrast to the absence of bone matrix, the cellular organization of the cartilage growth plate was normal in *Osx* null mutants except for the disordered organization of the deep layers of the zone of hypertrophic chondrocytes. Furthermore, Osx appeared to have no role in patterning of the skeleton. Indeed, at E12.5, a time when many of the patterning decisions of the embryonic skeleton have been made, *Osx* null embryos were indistinguishable from wild-type embryos. In addition, in newborn mutants, densely packed mesenchymal cells in membranous skeletal elements, unable to differentiate into osteoblasts, occupied the same space as that occupied by osteoblasts in wild-type embryos.

Osx Is a Novel Transcription Factor Belonging to the Sp/XKLF Family

Consistent with the phenotype of *Osx* null mutants, the *Osx* gene is expressed in all osteoblasts during mouse embryonic development. Osx contains a DNA binding domain consisting of three C2H2-type zinc fingers at its C terminus that share a high degree of identity with motifs in Sp1, Sp3, and Sp4. Somewhat less identity is shared with motifs in FKLF2 (Asano et al., 2000), BTEB1 (Imataka et al., 1992), and other members of the Krüppel-like factor family (Philipsen and Suske, 1999; Turner and Crossley, 1999). Osx binds to Sp1 and EKLF consensus sequences and to other G/C-rich sequences. Such G/C-rich sequences are present in many promoters, including those corresponding to the genes that are inactive in *Osx* null embryos (Hafner et al., 1995; Karsenty and de Crombrugghe, 1991; Ogata et al., 1997). Osx also contains a proline- and serine-rich transcription activation domain, as do several other members of the XKLF family (Philipsen and Suske, 1999). However, the amino acid sequence of Osx outside of its DNA binding domain shares no significant similarity with any other human, mouse, *Drosophila*, or *Caenorhabditis elegans* polypeptide. This is in agreement with the phenotype of *Osx* null mice, indicating that no other mouse protein can substitute for the function of Osx in osteoblast differentiation.

Osx Acts Downstream of Runx2/Cbfa1

Osteogenic cells of *Osx* null mutants that were completely blocked in their differentiation into osteoblasts expressed *Runx2/Cbfa1* at levels comparable to those in wild-type osteoblasts. Hence, Osx was not required for *Runx2/Cbfa1* expression. Since *Osx* was not expressed in *Runx2/Cbfa1*-defective embryos, we concluded that expression of *Osx* required Runx2/Cbfa1 and that Osx therefore acted downstream of Runx2/Cbfa1. Although Runx2/Cbfa1 is needed for *Osx* expression in osteogenic cells, Osx is not expressed in hypertrophic chondrocytes despite expression of *Runx2/Cbfa1* in these cells. The levels of Runx2/Cbfa1 may be insufficient in hypertrophic chondrocytes, and/or *Osx* expression may require additional transcription factors that are missing in hypertrophic chondrocytes.

The Phenotype of *Osx* Mutants Is Different than That of *Runx2/Cbfa1* Mutants

Although the phenotypes of *Osx* null and *Runx2/Cbfa1* null mutants are both characterized by a lack of bone formation and by an absence of differentiated osteoblasts, there are important differences in the phenotypes of these mutants. In the humerus and femur of *Runx2/Cbfa1* null mice, markers of hypertrophic chondrocytes are not expressed (Inada et al., 1999). In addition, in skeletal elements in which these markers are expressed, very little mineralization of the ECM of hypertrophic chondrocytes occurs in *Runx2/Cbfa1* null embryos, strongly suggesting that a mineralization defect exists in the endochondral skeleton of *Runx2/Cbfa1* null mice. Importantly, in *Runx2/Cbfa1* null embryos, no invasion of the matrix of hypertrophic chondrocytes by cells of the periosteum/perichondrium takes place, no osteoclasts/chondroclasts are found in the matrix, and no matrix degradation occurs (Komori et al., 1997). Notably, *Osx* was not expressed in hypertrophic chondrocytes in our study, and both the levels of expression of *Col10al* and *Ihh* and the aspect of hypertrophic chondrocytes

were normal in *Osx* null mutants. In addition, mineralization of the hypertrophic zone was much more pronounced in *Osx* null embryos than in *Runx2/Cbfa1* null embryos. It should also be noted that the abundant wedge-shaped mesenchyme in *Osx* null embryos contrasted with the thin mesenchyme in the periosteum in *Runx2/Cbfa1* null embryos.

Interestingly, ectopic expression of *Runx2/Cbfa1*, directed by *Col2a1* regulatory elements in *Runx2/Cbfa1* null embryos, leads to a partial rescue of the phenotype of *Runx2/Cbfa1* null embryos (Takeda et al., 2001). This partial rescue includes hypertrophic chondrocyte differentiation in endochondral skeletal elements in which such differentiation is defective in the parent *Runx2/Cbfa1* null embryos, VEGF expression by hypertrophic chondrocytes, vascular invasion of the zone of hypertrophic chondrocytes, and the presence of multinucleated TRAP-positive cells in the hypertrophic cartilage matrix. All these processes were absent in *Runx2/Cbfa1* null embryos. However, no bone formation and no osteoblast differentiation occurred in rescued embryos. Thus, Runx2/Cbfa1 has two very distinct functions in bone formation. First, it has an essential role in the differentiation of mesenchymal progenitors into osteoblasts in both the endochondral and membranous skeletons. The second function of Runx2/Cbfa1 is to stimulate hypertrophic chondrocyte differentiation. The phenotype of *Runx2/Cbfa1* null mice is the result of the abolition of both functions. In contrast, in *Osx* null embryos, the lack of bone formation appears to be caused entirely by an inability of osteoblasts to differentiate.

There are several possible explanations for the absent expression of almost all osteoblast marker genes in *Osx* null mutants, despite levels of expression of *Runx2/Cbfa1* that are comparable to those present in wild-type osteoblasts. Several of these marker genes contain Runx2/Cbfa1 binding sites in their promoters and mutations in these sites (Benson et al., 1999; Ducy et al., 1997; Sato et al., 1998), which abolished the binding of Runx2/Cbfa1, inhibited the activity of these promoters in transient expression experiments, consistent with the hypothesis that these genes might be direct targets of Runx2/Cbfa1. Although one cannot exclude that the in vivo function of Runx2/Cbfa1 to activate osteoblast marker genes is entirely mediated by Osx, we favor a model whereby several osteoblast marker genes need both Osx and Runx2/Cbfa1 for their expression. Others would require only Osx, whereas still other marker genes would require only Runx2/Cbfa1. It is further possible that for the expression of some osteoblast-specific genes, Osx is the only factor required but Runx2/Cbfa1 could increase the activity of these genes. Our in vitro experiments suggest that Osx is sufficient to activate the *osteocalcin* gene in both C2C12 and C3H10T1/2 cells. In addition, Osx is also sufficient to activate *Col1a1* gene in C2C12 cells.

Pathway of Osteoblast Differentiation

Our experiments suggest the following model for osteoblast differentiation. Osteoblast progenitors in mesenchymal condensations of both endochondral and membranous skeletal elements first differentiate through one or several steps into preosteoblasts; Runx2/Cbfa1 has an essential role in this process (Figure 7). These preosteoblasts do not express osteoblast marker genes. Because in both the membranous and endochondral skeletons, *Osx* null preosteoblasts, which are blocked from differentiating into osteoblasts, express several chondrocyte marker genes, including *Sox9*, *Sox5*, *Col2a1*, and *Ihh*, we postulate that preosteoblasts are still bipotential. This bipotentiality implies that the progenitors of these cells also have the potential to differentiate into osteoblasts and chondrocytes. In both endochondral and intramembranous skeletal elements, the *Runx2/Cbfa1*-expressing preosteoblasts then differentiate in one or more steps into mature osteoblasts and express characteristic osteoblast marker genes, a process that requires Osx. It is possible that Runx2/Cbfa1 and other transcription factors collaborate with Osx to activate these osteoblast marker genes in vivo to produce a bone-specific matrix.

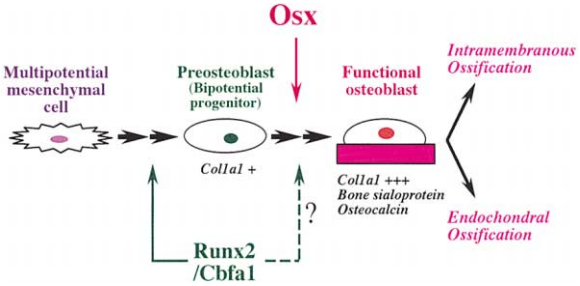

Figure 7. Model of Osteoblast Differentiation Pathway

Multipotential mesenchymal progenitors first differentiate into preosteoblasts, a process for which Runx2/Cbfa1 is needed. These preosteoblasts are still bipotential; i.e., they have the potential to differentiate into both osteoblast and chondrocytes. Preosteoblasts do not express osteoblast marker genes, except low levels of *Col1a1* typical of mesenchymal cells. Preosteoblasts then differentiate into functional osteoblasts expressing high levels of osteoblast marker genes. This process requires Osx.

Our experiments provide strong evidence supporting the hypothesis that osteoblasts and chondrocytes derive from a common precursor cell. Interestingly, the bipotentiality of the cells is maintained in *Runx2/Cbfa1*-expressing preosteoblasts that appear to be committed to the osteoblast lineage. We speculate that in osteoblasts, Osx might be a negative regulator of *Sox9* and *Sox5* expression, preventing these cells from choosing a chondrocyte differentiation pathway.

In summary, based on (1) the identification of Osx as a transcription factor that is essential for osteoblast differentiation, (2) the normal levels of expression of *Runx2/Cbfa1* in *Osx* null mutant preosteoblasts, and (3) the lack of *Osx* expression in *Runx2/Cbfa1* null mice, our results add a distinct step to the pathway of osteoblast differentiation.

Experimental Procedures

Generation and Genotyping of *Osx* Mutant Mice

Osx genomic clones were isolated from a mouse 129/SvEv genomic DNA library. The targeting vector was constructed by inserting an IRES-lacZ-polyA/loxP-flanked PGK neo-bpA cassette into the second coding exon of *Osx*. An MC1tkpA (tk) expression was induced for negative selection (Bi et al., 1999). AB-1 ES cell clones carrying

an *Osx* mutation were identified by Southern blot analysis using *Osx* probes located outside the region used for homologous recombination. Mouse chimeras were generated by injection of mutant ES cell clones into C57BL/6 blastocysts. Mutant mice were analyzed in the C57BL/6 X 129/SvEv mixed genetic background. Homozygous null mice derived from three independent ES cell clones exhibited identical phenotypes. Mice were genotyped using genomic DNA isolated from the tails digested with EcoRI or EcoRV and hybridized with an NheI-ScaI probe (5′ probe) or an Asp718-NheI probe (3′ probe). The wild-type and mutant alleles were detected as 12 kb and 5.7 kb fragments, respectively, with the 5′ probe and as 18 kb and 12 kb fragments, respectively, with the 3′ probe. PCR genotyping was performed using two sets of primers: Osx5 and Osx3 for the wild-type allele, and bpA and Osx3 for the mutant allele. Osx5/Osx3 primers and bpA/Osx3 primers yielded 286 bp and 395 bp PCR fragments, respectively.

Analyses of Mutant Mice

Whole-mount X-gal staining of embryo and alcian blue and alizarin red staining of skeleton were performed as described (Hogan et al., 1994). For histological analysis, paraformaldehyde-fixed, paraffin-embedded embryonic undecalcified tissue sections were stained with alcian blue, hematoxylin, and Treosin (StatLab). To detect mineral deposition, tissue sections were stained with von Kossa's method followed by nuclear fast red counter staining. TRAP staining was performed using a leucocyte acid phosphatase kit (Sigma). Immunodetection of MMP-9 and cathepsin K were performed using anti-MMP-9 (Chemicon) and anti-cathepsin K (Santa Cruz Biotechnology) antibodies with a standard protocol (Ausubel et al., 1995).

Acknowledgments

We are grateful to Michael J. Owen and Rena d'Souza for providing sections of *Runx2/Cbfa1*-null mutants, to Heidi Eberspaecher and Hui Dai for technical support, to Jinkun Chen, Véronique Lefebvre, Andrew P. McMahon, and Genetics Institute for reagents, and to Sanker Maity, Shunichi Murakami, Véronique Lefebvre, and Haruhiko Akiyama for helpful discussions. We thank William H. Klein and Randy L. Johnson for their comments on the manuscript. We also thank Janie Finch for editorial assistance. This work was funded by NIH grants P01 AR42919 (to B.d.C. and R.R.B.). DNA sequencing was performed by the University of Texas M. D. Anderson Cancer Center core sequencing facility, which is supported by NCI grant CA 16672.

Received July 27, 2001; revised December 5, 2001.

References

Asano, H., Li, X.S., and Stamatoyannopoulos, G. (2000). FKLF-2: a novel Kruppel-like transcriptional factor that activates globin and other erythroid lineage genes. Blood *95*, 3578–3584.

Ausubel, F., Brent, R., Kingston, R.E., Moore, D.D., Seidman, J.G., Smith, J.A., and Struhl, K. (1995). Short Protocols in Molecular Biology, 3rd Edition (New York: John Wiley & Sons, Inc.).

Benson, M.D., Aubin, J.E., Xiao, G., Thomas, P.E., and Franceschi, R.T. (1999). Cloning of a 2.5 kb murine bone sialoprotein promoter fragment and functional analysis of putative Osf2 binding sites. J. Bone Miner. Res. *14*, 396–405.

Black, B.L., and Olson, E.N. (1998). Transcriptional control of muscle development by myocyte enhancer factor-2 (MEF2) proteins. Annu. Rev. Cell Dev. Biol. *14*, 167–196.

Bi, W., Deng, J.M., Zhang, Z., Behringer, R.R., and de Crombrugghe, B. (1999). Sox9 is required for cartilage formation. Nat. Genet. *22*, 85–89.

Bilezikian, J.P., Raisz, L.G., and Rodan, G.A. (1996). Principles of Bone Biology (San Diego, CA: Academic Press, Inc.).

Chen, J., Shapiro, H.S., and Sodek, J. (1992). Development expression of bone sialoprotein mRNA in rat mineralized connective tissues. J. Bone Miner. Res. *7*, 987–997.

DeLise, A.M., Fischer, L., and Tuan, R.S. (2000). Cellular interactions and signaling in cartilage development. Osteoarthritis Cartilage *8*, 309–334.

Ducy, P., Zhang, R., Geoffroy, V., Ridall, A.L., and Karsenty, G. (1997). Osf2/Cbfa1: a transcriptional activator of osteoblast differentiation. Cell *89*, 747–754.

Fang, J., and Hall, B.K. (1997). Chondrogenic cell differentiation from membrane bone periostea. Anat. Embryol. *196*, 349–362.

Gashler, A.L., Swaminathan, S., and Sukhatme, V.P. (1993). A novel repression module, an extensive activation domain, and a bipartite nuclear localization signal defined in the immediate-early transcription factor Egr-1. Mol. Cell. Biol. *13*, 4556–4571.

Gowen, M., Lazner, F., Dodds, R., Kapadia, R., Feild, J., Tavaria, M., Bertoncello, I., Drake, F., Zavarselk, S., Tellis, I., et al. (1999). Cathepsin K knockout mice develop osteopetrosis due to a deficit in matrix degradation but not demineralization. J. Bone Miner. Res. *14*, 1654–1663.

Hafner, M., Zimmermann, K., Pottgiesser, J., Krieg, T., and Nischt, R. (1995). A purine-rich sequence in the human BM-40 gene promoter region is a prerequisite for maximum transcription. Matrix Biol. *14*, 733–741.

Hogan, B., Beddington, R., Costantini, F., and Lacy, E. (1994). Manipulating the Mouse Embryo, 2nd Edition (Cold Spring Harbor, NY: Cold Spring Harbor Laboratory Press).

Imataka, H., Sogawa, K., Yasumoto, K., Kikuchi, Y., Sasano, K., Kobayashi, A., Hayami, M., and Fujii-Kuriyama, Y. (1992). Two regulatory proteins that bind to the basic transcription element (BTE), a GC box sequence in the promoter region of the rat P-4501A1 gene. EMBO J. *11*, 3663–3671.

Inada, M., Yasui, T., Nomura, S., Miyake, S., Deguchi, K., Himeno, M., Sato, M., Yamagiwa, H., Kimura, T., Yasui, N., et al. (1999). Maturational disturbance of chondrocytes in Cbfa1-deficient mice. Dev. Dyn. *214*, 279–290.

Johnson, R.L., and Tabin, C.J. (1997). Molecular models for vertebrate limb development. Cell *90*, 979–990.

Karsenty, G. (1999). The genetic transformation of bone biology. Genes Dev. *13*, 3037–3051.

Karsenty, G., and de Crombrugghe, B. (1991). Conservation of binding sites for regulatory factors in the coordinately expressed alpha 1 (I) and alpha 2 (I) collagen promoters. Biochem. Biophys. Res. Commun. *177*, 538–544.

Katagiri, T., Yamaguchi, A., Komaki, M., Abe, E., Takahashi, N., Ikeda, T., Rosen, V., Wozney, J.M., Fujisawa-Sehara, A., and Suda, T. (1994). Bone morphogenetic protein-2 converts the differentiation pathway of C2C12 myoblasts into the osteoblast lineage. J. Cell Biol. *127*, 1755–1766.

Kim, I.S., Otto, F., Zabel, B., and Mundlos, S. (1999). Regulation of chondrocyte differentiation by Cbfa1. Mech. Dev. *80*, 159–170.

Komori, T., Yagi, H., Nomura, S., Yamaguchi, A., Sasaki, K., Deguchi, K., Shimizu, Y., Bronson, R.T., Gao, Y.H., Inada, M., et al. (1997). Targeted disruption of Cbfa1 results in a complete lack of bone formation owing to maturational arrest of osteoblasts. Cell *89*, 755–764.

Ogata, Y., Niisato, N., Furuyama, S., Cheifetz, S., Kim, R.H., Sugiya, H., and Sodek, J. (1997). Transforming growth factor-beta 1 regulation of bone sialoprotein gene transcription: identification of a TGF-beta activation element in the rat BSP gene promoter. J. Cell. Biochem. *65*, 501–512.

Olsen, B.R., Reginato, A.M., and Wang, W. (2000). Bone development. Annu. Rev. Cell Dev. Biol. *16*, 191–220.

Otto, F., Thornell, A.P., Crompton, T., Denzel, A., Gilmour, K.C., Rosewell, I.R., Stamp, G.W., Beddington, R.S., Mundlos, S., Olsen, B.R., et al. (1997). Cbfa1, a candidate gene for cleidocranial dysplasia syndrome, is essential for osteoblast differentiation and bone development. Cell *89*, 765–771.

Philipsen, S., and Suske, G. (1999). A tale of three fingers: the family of mammalian Sp/XKLF transcription factors. Nucleic Acids Res. *27*, 2991–3000.

Rosen, E.D., and Spiegelman, B.M. (2000). Molecular regulation of adipogenesis. Annu. Rev. Cell Dev. Biol. *16*, 145–171.

Sato, M., Morii, E., Komori, T., Kawahata, H., Sugimoto, M., Terai, K., Shimizu, H., Yasui, T., Ogihara, H., Yasui, N., et al. (1998). Transcriptional regulation of osteopontin gene in vivo by PEBP2alphaA/CBFA1 and ETS1 in the skeletal tissues. Oncogene *17*, 1517–1525.

Smits, P., Li, P., Mandel, J., Zhang, Z., Den, J.M., Behringer, R.R., de Crombrugghe, B., and Lefebvre, V. (2001). The transcription factor L-Sox5 and Sox6 are essential for cartilage formation. Dev. Cell *1*, 277–290.

St-Jacques, B., Hammerschmidt, M., and McMahon, A.P. (1999). Indian hedgehog signaling regulates proliferation and differentiation of chondrocytes and is essential for bone formation. Genes Dev. *13*, 2072–2086.

Takeda, S., Bonnamy, J.P., Owen, M.J., Ducy, P., and Karsenty, G. (2001). Continuous expression of Cbfa1 in nonhypertrophic chondrocytes uncovers its ability to induce hypertrophic chondrocyte differentiation and partially rescues Cbfa1-deficient mice. Genes Dev. *15*, 467–481.

Tickle, C. (1995). Vertebrate limb development. Curr. Opin. Genet. Dev. *5*, 478–484.

Turner, J., and Crossley, M. (1999). Mammalian Krüppel-like transcription factors: more than just a pretty finger. Trends Biochem. Sci. *24*, 236–240.

Ueta, C., Iwamoto, M., Kanatani, N., Yoshida, C., Liu, Y., Enomoto-Iwamoto, M., Ohmori, T., Enomoto, H., Nakata, K., Takada, K., et al. (2001). Skeletal malformations caused by overexpression of Cbfa1 or its dominant negative form in chondrocytes. J. Cell Biol. *153*, 87–100.

Vu, T.H., Shipley, J.M., Bergers, G., Berger, J.E., Helms, J.A., Hanahan, D., Shapiro, S.D., Senior, R.M., and Werb, Z. (1998). MMP-9/gelatinase B is a key regulator of growth plate angiogenesis and apoptosis of hypertrophic chondrocytes. Cell *93*, 411–422.

Accession Numbers

The GenBank accession number for the mouse Osterix reported in this paper is AF184902.